ELSEVIER

Available online at www.sciencedirect.com

SCIENCE DIRECT®

Applied Surface Science 216 (2003) 436–446

applied surface science

www.elsevier.com/locate/apsusc

Understanding the growth mechanisms of GaAs and InGaAs thin films by employing first-principles calculations

P. Kratzer*, E. Penev, M. Scheffler

Fritz-Haber-Institut der Max-Planck-Gesellschaft, Faradayweg 4–6, 14195 Berlin-Dahlem, Germany

Abstract

We demonstrate the use of density-functional theory (DFT) calculations for understanding molecular beam epitaxy (MBE) of GaAs and InGaAs films at the atomic level. For analyzing island growth in homoepitaxy of GaAs(0 0 1), the use of DFT in conjunction with kinetic Monte Carlo (kMC) simulations is discussed. This approach enables us to elucidate the growth mechanisms of islands on the $\beta 2(2 \times 4)$-reconstructed surface and to compute the saturation values of the island density. Furthermore, DFT calculations are employed to investigate the stability of ultrathin InGaAs films on GaAs(0 0 1) as a function both of the chemical potential of arsenic in the growth environment, and of mechanical strain. Under very As-rich conditions, for deposition of two-thirds of a monolayer (ML) of InAs, our calculations indicate the formation of a (2×3)-reconstructed InGaAs(0 0 1) surface alloy. The calculated atomic structure is in excellent agreement with X-ray diffraction data. For less As-rich conditions and larger amounts of deposited InAs, we find InGaAs films with a $\alpha 2(2 \times 4)$ reconstruction to be most favorable.
© 2003 Elsevier Science B.V. All rights reserved.

PACS: 68.55.-a; 81.15.Aa

Keywords: Growth simulations; Epitaxy; Formation kinetics of thin films; Diffusion and interface mixing

1. Introduction

Heterostructures grown from III–V compound materials have been playing an important role in semiconductor physics in the last 20 years, and have recently found numerous applications in semiconductor devices, in particular in high-frequency and optoelectronic applications. The success of these heterostructures owes much to the capability to grow samples in a controlled way, by molecular beam epitaxy (MBE) and metal-organic vapor-phase epitaxy (MOVPE). Growth conditions can be chosen in a way to yield samples with specific features, e.g. very smooth films for quantum-well structures with high electron mobility. Moreover, the spontaneous formation of nanostructures in heteroepitaxy under suitably chosen growth conditions has recently attracted enormous interest. These nanostructures, after being overgrown with a capping layer, can be employed as quantum dots that confine carriers on the nanometer scale. In this way, samples with unusual electronic or optical properties can be realized, and one may even hope to use these nanostructures in computing devices which employ quantum effects as deliberate part of their design. These developments have raised the desire to

* Corresponding author. Tel.: +49-30-8413-4809; fax: +49-30-8413-4701.
E-mail address: kratzer@fhi-berlin.mpg.de (P. Kratzer).
URL: http://www.fhi-berlin.mpg.de/th/member/kratzer_p.html.

0169-4332/03/$ – see front matter © 2003 Elsevier Science B.V. All rights reserved.
doi:10.1016/S0169-4332(03)00392-1

understand and possibly control growth even better, i.e. on the atomic scale.

Despite the technological importance of these growth techniques, our understanding of the processes involved on the atomic scale is still in its infancy. Here, atomistic calculations on the basis of density-functional theory (DFT) can provide important new insight. One way of making this computational tool useful for application-oriented research is by employing ab initio thermodynamics to study heteroepitaxial films on a substrate of different lattice constant. Furthermore, it is possible to perform simulations using the realistic atomic structure of the surface, and to study the motion of particles and its associated energetics, i.e. binding energies and energy barriers. Moreover, when combined with the kinetic Monte Carlo (kMC) technique, the DFT calculations can provide information on how the barriers for molecular processes, such as adatom diffusion, desorption, attachment to, and detachment from islands, affect the growth morphology of thin films.

The investigations reported here focus on MBE of the technologically important material system InAs/GaAs. Before describing the results of our calculations, we shall briefly review the experimental setup in MBE: in an ultra-high vacuum chamber, sources of Ga or In atoms and arsenic molecules are used to deposit thin films on a substrate, a GaAs wafer, usually with surface orientation (0 0 1). In our modeling, we consider the situation were As_2 molecules are used as source of arsenic. In the experiments, both As_2 and As_4 molecular sources are in use. Differences in the growth morphology for the two molecular species have been reported (i.e. difference in island densities, see [1]), but many aspects of growth are similar in both cases. As a possible explanation for the similarities, we mention that As_4 is likely to be broken up into As_2 molecules when coming in contact with certain reactive sites on the surface [2]. In the temperature range most commonly used in MBE, the species desorbing from the surfaces is predominantly As_2.

Of the three species Ga, In and As, arsenic is the most volatile one, desorbing from the surface already at modest temperatures. Temperature programmed desorption (TPD) spectra show peaks at various temperatures which are attributed to surface reconstructions with different stoichiometry [3]. The α and β peaks associated with desorption of As_2 occur at $T = 840$ and 750 K, respectively. For InAs, the temperatures associated with different peaks in the TPD spectrum of As_2 molecules are somewhat lower [4], with the main peak at around 700 K, in accordance with the smaller cohesive energy of this compound as compared to GaAs.

In ternary $In_xGa_{1-x}As$ compounds, indium has a tendency to segregate towards the surface. This is in agreement with the lower calculated surface energy of InAs as compared to GaAs [5,6]. As a first approximation, we note that the surface energies of InAs and GaAs follow the same trend as the cohesive energy of these two materials. Switching from the most As-rich to cation-rich conditions, which corresponds to increasing temperature in the TPD spectra, the GaAs(0 0 1) surface displays a sequence of reconstructions, from $c(4 \times 4)$ over $\beta2(2 \times 4)$ and $\alpha2(2 \times 4)$ to the $\zeta(4 \times 2)$ structure. There is ample support for this sequence, both experimentally and from DFT calculations (see, for example [7,8] and references therein). For InAs(0 0 1), the $c(4 \times 4)$ reconstruction is only marginally stable as indicated by our calculations [9]. Also, X-ray diffraction data are available in support of the assignment of the In-rich (4×2) structure with a variant of the ζ reconstruction [10].

In this contribution, we attempt to give a brief summary of what is known about the development of thin films through various stages of their deposition. First, we will review results about the atomic processes relevant for island nucleation on the substrate during the early stage of deposition. Secondly, we will present some new computational results for ultrathin films of InAs on GaAs for sub-monolayer deposition. Finally, we will discuss the evolution of these films for thicknesses exceeding one monolayer (ML).

2. Methodology

2.1. DFT calculations

The computational method [11] employed in this study uses norm-conserving pseudopotentials in conjunction with a plane-wave basis set (cutoff energy of 10 Ry). Calculations were performed both within the local-density approximation (LDA) to exchange and correlation, and with a gradient-corrected density

functional (PBE [12]). Surfaces were represented, within the supercell approach, by slabs whose bottom (cation-terminated) surface was passivated by fractionally charged H atoms ($Z = 1.25$). Summation over the Brillouin zone was carried out using a set of k points equivalent to a density of 64 points or higher in the 1×1 surface Brillouin zone. The GaAs lattice constant calculated in LDA is about 2% smaller than the experimental lattice constant, and about 2% too large in PBE. For InAs, the lattice constant in LDA closely matches the experimental one, while PBE yields a lattice constant more than 4% too large. The relative stability of different surface reconstructions is similar in LDA and PBE, and the same qualitative picture emerges. In this paper, we chose to present LDA surface energies. The binding energies of atoms and molecules to the surface are overestimated in LDA, while the PBE values are in better agreement with the experimentally reported desorption temperatures of the various species. For the kinetic simulations, we therefore use binding energies and energy barriers obtained within PBE.

2.2. Thermodynamic approach

For the coexistence of a ternary solid compound with its vapor, Gibbs phase rule states that there are two thermodynamic variables, in addition to temperature, T, and total pressure, p, that describe the chemical environment in which the equilibrium is established. These could be, for instance, the partial pressures of two of the constituent elements. However, it is often more convenient to work with chemical potentials as thermodynamic variables. Since the surface free energy is defined as the difference of the free energies of a slab calculation and bulk calculations, contributions due to finite-temperature effects tend to cancel. Hence, to a good approximation, surface free energies can be obtained from total energy differences at $T = 0$ K. If we can neglect the small pressure dependence due to the compressibility of the solid, and rely on error cancellation for the vibrational contributions to the free energy, it is possible to absorb all dependencies on p and T into an implicit dependence of the chemical potential(s) on these variables.

Since As_2 is a quite volatile species, a solid of $In_xGa_{1-x}As$ exchanges readily arsenic with its environment through adsorption and desorption of As molecules. Therefore we have a physical motivation for choosing one of the free thermodynamic variables to be the arsenic chemical potential μ_{As}, thereby making use of the observation that, among the three species in question, it is arsenic for which the partial equilibrium between solid and vapor is most easily established. For the In and Ga species, on the other hand, desorption can be kept negligibly small at typical MBE temperatures, e.g. below 0.03 ML/s for In up to $T = 820$ K, and below 0.06 ML/s for Ga up to $T = 920$ K [13].

Here we deal with substrates consisting of pure GaAs. When InAs is deposited on such a substrate, the In atoms will remain in the atomic layers at, or at least close to the surface. Therefore the deposited amount of In, or the indium coverage θ_{In}, is a well-defined quantity. Hence we prefer to choose θ_{In}, rather than μ_{In}, as the second thermodynamic variable in the phase equilibrium under study. Note that this treatment implies the chemical potential for Ga atoms to be fixed at the value that corresponds to chemical equilibrium with the bulk GaAs for the given value of μ_{As}. Within the approximation that finite-temperature contributions to the surface free energy cancel each other, we evaluate all its contributions at $T = 0$ K. For the In atoms deposited at the surface, we use the cohesive energy of InAs at $T = 0$ K as energy reference. This leads to the expression for the surface free energy

$$\gamma_f(\mu_{As}) = [E_{tot} - N_{Ga}E^{coh}_{GaAs} - N_{In}E^{coh}_{InAs} - (N_{As} - N_{Ga} - N_{In})(\mu_{As} - \mu_{As(bulk)})]/A \quad (1)$$

Here E_{tot} is the total cohesive energy of the slab calculated within DFT, and approximated by its value at $T = 0$ K; E^{coh}_{InAs} and E^{coh}_{GaAs} the cohesive energies of the respective bulk phases, also at $T = 0$ K; N_{Ga}, $N_{In} = \theta_{In}A$, and N_{As} the numbers of Ga, In and As atoms in the unit cell, respectively; and A is its area.

2.3. Kinetic approach

For analyzing the surface morphology that evolves *during* growth, it is usually not sufficient to calculate thermodynamic equilibrium properties. Rather, we need to study the steady state of a system where (at least some of) the intermediate configurations are not fully equilibrated. To investigate the kinetics of such a

system, knowledge of the *rate constant* Γ for all the processes involved is required. While it is often very difficult to derive these data from experiments, DFT calculations give access to the rate constants by calculating the energy barrier ΔE associated with individual atomic processes, using the Arrhenius expression for the rate constant of an activated process, $\Gamma = \Gamma_0 \exp(-\Delta E/k_B T)$. With this knowledge as a starting point, it is possible to build up a model of growth which rests on valid atomistic input.

In the above paragraph, we had stated that the concentration of arsenic species on the surface is close to the value dictated by thermal equilibrium between the vapor and the GaAs bulk phase on typical time scales of growth (of the order of seconds). This means that both adsorption and desorption processes of arsenic molecules, which are treated explicitly in the kinetic approach, are frequent events. Hopping processes of adatoms between adsorption sites have an even lower energy barrier ΔE than As_2 desorption, and thus occur even more frequently. However, island nucleation as well as growth of existing islands involve *surface chemical reactions* of Ga atoms and As_2 molecules, which are specific to the surface site where they take place. Equilibrium is not reached on the time scale of these reactions. Hence the density and other properties of islands, such as their size distribution and shape, are kinetically controlled quantities, and we need to follow the molecular processes in detail to understand how they evolve. kMC simulations are an excellent tool to study the host of molecular processes, including their interdependence, which all together determine the kinetically controlled properties.

3. Atomistic studies of island nucleation in MBE

As an example for a system where the molecular processes of growth have been thoroughly investigated, we discuss homoepitaxy of GaAs on GaAs(0 0 1). Under most frequently used MBE conditions, this surface displays the β2(2 × 4) reconstruction [14–16]. Hence the substrate is not atomically flat, but exposes three layers of atoms at the surface. Each (2 × 4) unit cell is built up from two As dimers and two missing dimers in the topmost layer, and a missing Ga pair in the second layer. The missing atoms leave room for 'trenches' running in the $[\bar{1}\,1\,0]$ direction separated by 'hills' of adjacent As dimers in the top layer. In the trenches, As atoms of the third layer are exposed, which also form As dimers (see Fig. 1a).

Both Ga atoms and As_2 molecules are supplied simultaneously by molecular beams. We consider growth conditions with a supply of arsenic sufficiently high to stabilize the β2-reconstruction during growth. Due to its hill-and-trench structure, the β2-reconstruction enables adsorption of both Ga atoms and As_2 molecules, and thus can reproduce itself locally in the newly grown layer. In contrast to this growth mode, Ishii and Kawamura [17] have suggested a growth model in which the surface structure oscillates during growth between a Ga-rich and an As-rich surface termination in different parts of the surface. This scenario may be appropriate for growth at very high temperatures or low As supply.

For growth on the β2-surface, due to the complexity of this reconstruction, it is required to consider more than 30 different types of processes to obtain an appropriate picture of growth. For example, diffusion of a single Ga adatom is governed by the interplay of 10 different processes. As a result, Ga diffusion is anisotropic with an activation energy of 0.8 eV in the [1 1 0] direction, and 0.7 eV along the trenches in $[\bar{1}\,1\,0]$ direction (see Table 1). Furthermore, the simulations include reactions of Ga with the As dimers of the surface reconstruction, thereby splitting the dimer bond, attachment and detachment of Ga at island edges, and adsorption and desorption of As_2. For the adsorption of As_2, both experiment [18] and calculations [19] have pointed out the importance of a weakly bound precursor state. As_2 molecules temporarily trapped in this state explore numerous surface sites before they either encounter a reactive site with a Ga adatom suitable for adsorption, or else eventually desorb. The As_2 flux relevant for the kMC simulation

Table 1
Activation energy (in eV) for surface diffusion of Ga for homoepitaxy on in GaAs(0 0 1), and of In on the heteroepitaxial $In_{2/3}Ga_{1/3}As$(0 0 1) film shown in Fig. 3b

Adatom/substrate	Direction	
	$[\bar{1}\,1\,0]$	[1 1 0]
Ga/GaAs(0 0 1)–β2(2 × 4)	0.7	0.8
In/$In_{2/3}Ga_{1/3}As$(0 0 1)–(2 × 3)	0.13	0.29

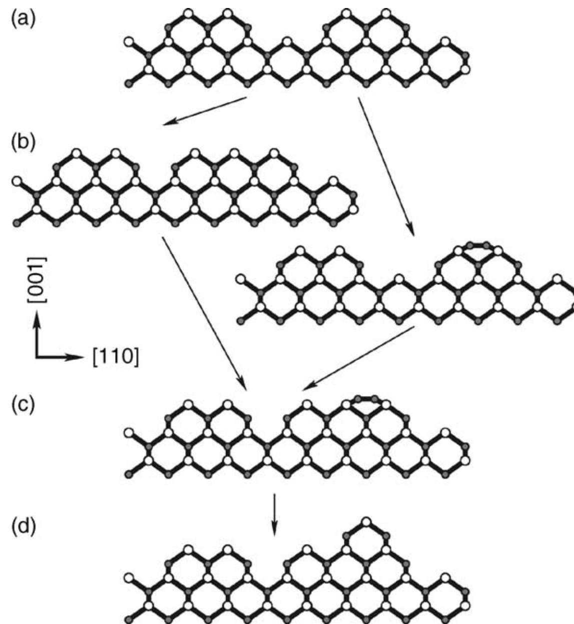

Fig. 1. Schematic representation of the growth mechanism in GaAs homoepitaxy on the GaAs(0 0 1)–β2 surface (side view). (a) The substrate is corrugated on the atomic scale, with 'hills' of As dimers (open circles, dimer axis perpendicular to the plane of the graph) and 'trenches'. Ga atoms (filled circles) with dangling bonds appear at the 'sidewalls' of the trenches. (b) Left: attachment of material in the trench, yielding a local β1-reconstruction; right: Ga dimer as a metastable growth intermediate. (c) Formation of a Ga dimer adjacent to locally filled trench. (d) The island extends into a new layer after As_2 adsorption.

is not given by the direct flux from the beam source, but rather by the density of molecules in the precursor state, times the frequency with which they probe a surface site. We estimate this effective flux by $F^{\mathrm{eff}}_{\mathrm{As}_2} = p\exp[(E_{\mathrm{B}}/k_{\mathrm{B}}T) - 1]/\sqrt{2mk_{\mathrm{B}}T}$ assuming equilibrium between the precursor and the gas phase. Here, p is the beam-equivalent pressure of As_2, and $E_{\mathrm{B}} \sim 0.3$ eV is a typical binding energy in the potential well of the precursor. The resulting effective flux is a factor 50–100 higher than the direct flux at typical growth temperatures, i.e. an As_2 molecule probes on average about 50–100 surface sites during its lifetime in the precursor.

Performing kMC simulations using the rates obtained from the DFT calculations, we are able to extract the essential sequence of processes that give rise to island growth on the GaAs(0 0 1)–β2 substrate [20]. Furthermore, the DFT calculations enable us to identify metastable configurations that appear as intermediates [21]. Such metastable intermediates are shown in Fig. 1. By attachment of material in the trenches, two Ga atoms and a third As dimer are added to the β2-reconstruction, yielding a unit cell with local β1-reconstruction (Fig. 1b, left part). If the rate of desorption of arsenic exceeds adsorption (i.e. when growing at high temperatures and under low As fluxes), the Ga adatoms agglomerate into Ga dimers (Fig. 1b, right part). The formation of these Ga dimers occurs preferentially near sites where material has already been filled into the trenches, i.e. where the local β1-reconstruction has appeared (Fig. 1c). Finally, if two or more such Ga dimers have formed at sites adjacent in the $[\bar{1}\,1\,0]$ direction, these offer favorable adsorption sites for As_2 molecules, and adsorption of As_2 completes growth of a nucleus that now extends into the new layer (Fig. 1d). As a result of this growth mechanism, islands are elongated along the $[\bar{1}\,1\,0]$ direction. Experimental studies in combination with modeling have demonstrated that these islands, once they grow larger, exhibit again the well-known β2-reconstruction pattern [22]. As an explanation, it has been pointed out that the binding energy of As dimers is site-selective: if three or more As dimers are adjacent in the [1 1 0] direction, their

binding is weakened by a net repulsion [23,24]. Moreover, As_2 molecules do not adsorb in a layer filling the gap consisting of only a *single* vacancy (like in the β1-reconstruction, Fig. 1b, left part); the binding energy at these sites is too low [21]. In summary, the substrate acts as a template for the formation of islands in a new layer. The islands are oriented along the trenches of the substrate, and the β2-reconstruction is propagated into the newly grown layer.

While experimental studies of MBE growth on GaAs(0 0 1)–β2 are usually performed only in a rather narrow temperature interval where the substrate surface can be stabilized by working at a suitable Ga:As flux ratio, the kMC simulations are able to cover a much wider range of temperatures. The simulations find that the island density is non-monotonic as a function of temperature when studied in a wider range of $500\,K < T < 900\,K$ (see Fig. 2). This finding, which is rather unexpected from the point of view of 'standard' nucleation theory, is due to the crucial role of arsenic adsorption and desorption during growth. At $T \geq 800\,K$, desorption of As_2 becomes appreciable. Consequently, the attachment of material to the edges of existing islands, which involves the incorporation of arsenic, must be considered reversible

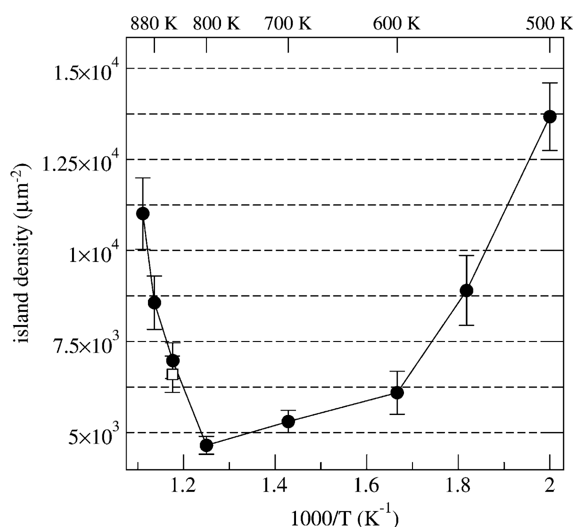

Fig. 2. Island number density for GaAs homoepitaxy after deposition for 1 s, Ga flux 0.1 ML/s and an effective As_2 flux of 100 ML/s. The filled circles are results of kMC simulations by the authors [20], the open square symbol is the measured island density from [1], at a Ga flux of 0.1 ML/s and a (direct) As_2 flux of 0.8 ML/s.

Table 2
Dependence of the island density n_{isl} calculated with a statistical uncertainty of ±10%, on the effective arsenic flux $F^{eff}_{As_2}$ for Ga flux of 0.1 ML/s and growth temperature $T = 700$ K

$F^{eff}_{As_2}$ (ML/s)	n_{isl} (μm^{-2})
3	2400
10	3000
30	3500
100	5300
300	4800
1000	4900

at these high temperatures. This leads to a change in the growth kinetics and to an increase in the nucleation of new islands [20,25]. As can be seen from Table 2, the results depend only weakly on the arsenic flux. In the range considered, the island density first increases with increasing arsenic flux, in agreement with experiment [1], and then saturates.

4. Ultrathin pseudomorphic films of InAs on GaAs

Experimentally, it has been demonstrated that island growth of InAs on the GaAs(0 0 1)–β2(2 × 4) proceeds in a qualitatively similar way to homoepitaxy of GaAs [26]. Of course, there are quantitative differences; in particular, the island density is lower for InAs, because of the different values for diffusion, attachment and desorption barriers for In atoms, and different activation energies for desorption of As_2 from InAs. In addition, one would expect heteroepitaxial strain to have some effect on growth. Indeed this effect leads to drastic changes in the growth morphology for deposition of >1 ML [27], but it is apparently less important for island nucleation and growth in the sub-monolayer regime.

However, more typical than deposition on GaAs(0 0 1)–(2 × 4) is the deposition of InAs on the c(4 × 4)-reconstructed GaAs(0 0 1) substrate, which is characteristic of growth at somewhat lower temperatures (corresponding to more As-rich conditions). Detailed reflection high-energy electron diffraction (RHEED) measurements by Belk et al. [28] show that even very small InAs coverages deposited on this substrate affect the surface morphology

strongly. A prominent feature of the surface morphology after InAs deposition is the formation of a wetting layer (WL) with both commensurate and incommensurate (1 × 3) and (2 × 3) reconstruction patterns. Similar results were also found by reflectance anisotropy spectroscopy [29,30]. We shall show here that formation of a surface alloy is the driving force for this structural transformation, and that the triple periodicity can be explained by it.

Unlike for pure GaAs(0 0 1) and pure InAs(0 0 1) surfaces, the structural information about the WL is very scarce. We start our DFT study by identifying a set of favorable structural models for the WL surface for a fixed coverage $\theta_{In} = 2/3$, without making any *a priori* assumption for the surface charge compensation. The triple-period (commensurate) reconstructions considered here are shown in Fig. 3. While never observed for the clean binary III–V(0 0 1) surfaces, a (2 × 3) reconstruction, Fig. 3b, for example, was reported for pseudomorphic InAs films grown on GaAs or InGaAs substrates [31,32]. For a $In_xGa_{1-x}As$(0 0 1) surface alloy, Sauvage-Simkin et al. [33] have demonstrated by X-ray diffraction that In–Ga ordering stabilizes the

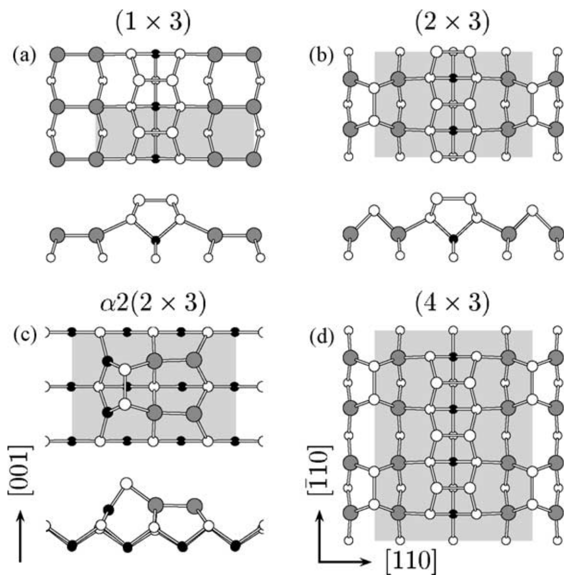

Fig. 3. Structural models for the commensurate ($n \times 3$) reconstructions of the $In_xGa_{1-x}As$(0 0 1) surface. Shaded polygons represent the surface unit cell. Atomic arrangement is indicated for atoms in the topmost four atomic layers (In: gray circles; Ga: black circles; As: open circles). Side views are shown in the lower parts of panels (a)–(c); the side view of (d) is identical to that in (b).

(2 × 3) reconstruction under As-rich conditions leading to $x = 2/3$. Subsequent diffraction experiments [34,35] confirmed their proposed structural model, Fig. 3b. The (1 × 3) model, Fig. 3a, is simply derived from (2 × 3) by removing the As dimers bonded to the third-layer In atoms, and dimerizing the latter in [1 1 0] direction. The α2(2 × 3) reconstruction is similar to the α2(2 × 4) for the clean binary surfaces: the second-layer dimers along [1 1 0] are formed by In, and no trench dimers are present giving the triple periodicity in this direction. The (4 × 3) model is obtained from (2 × 3) by removing every fourth As dimer from the continuous dimer row in the topmost layer leading to doubled period in [1̄ 1 0] direction. Some limited discussion of these models was given in [36–38]. The set is further augmented by including the α2(2 × 4) and β2(2 × 4) reconstructions. We have found [9] that on InAs(0 0 1) isotropic compressive strain favors exclusively the α2(2 × 4) reconstruction. A detailed analysis of the β2(2 × 4)-reconstructed WL was performed recently by Wang et al. [39,40] employing very similar computational settings.

Note that none of the ($n \times 3$) models obeys the electron counting rule (ECR) [41], which is often considered as an empirical heuristic principle for selecting probable atomistic models of reconstructed III–V semiconductor surfaces. Theoretically, it is the minimal property of the surface formation energy γ_f that determines which one out of a set of plausible reconstructions will be observed in *thermodynamic equilibrium*. To pursue this problem, we calculate γ_f of the WL (at zero temperature and pressure) for a reference thickness of $\theta_{In} = 2/3$ ML. This choice is dictated by the experimental observation that only for In composition $x = 2/3$ (for $\theta_{In} < 1$ ML we have $\theta_{In} \equiv x$) the triple-period reconstruction is commensurate [33,35]. The computational procedure has been discussed in detail in [9,40,42]. At fixed θ_{In}, for non-stoichiometric surfaces (here all except α2(2 × 4)) the surface free energy depends on μ_{As}, $\gamma_f = \gamma_f(\mu_{As})$. In order to define the most As-rich conditions possible, any excess As atoms are considered to be in equilibrium with a reservoir of bulk As in the rhombohedral A7 structure. Variation of μ_{As} is thus limited to the thermodynamically allowed range, $-|\Delta H_f| \leq \mu_{As} - \mu_{As(bulk)} \leq 0$, where $\Delta H_f = -0.68$ eV/atom is the calculated enthalpy of formation of bulk GaAs. The γ_f–μ_{As} diagram is shown in Fig. 3a.

There are a few interesting features to be pointed out for γ_f of the pseudomorphic $In_{2/3}Ga_{1/3}As(0\,0\,1)$ film. Under As-rich conditions none of the reconstructions considered can compete in terms of stability with the (2×3) model. Importantly, within the computational accuracy of ± 1 meV/Å^2, $In_{2/3}Ga_{1/3}As(0\,0\,1)$–$(2 \times 3)$ is energetically degenerate to the bare GaAs(0 0 1)–c(4×4) substrate for $\mu_{As} \rightarrow \mu_{As(bulk)}$ (stoichiometries of these reconstructions defer by only $\simeq 7\%$). However, with the μ_{As} decreasing, the α2(2×4) reconstruction becomes the most favorable, and at the $(2 \times 3) \rightarrow$ α2(2×4) transition the β2(2×4) phase appears to be nearly degenerate in energy. The low γ_f of the (2×3) reconstruction is somewhat unexpected as it violates the ECR. This surface, however, exhibits a strong tendency towards dimerization, leading to one dangling bond per 1×1 area. Recently it has been demonstrated [43] that the minimization of the number of dangling bonds is more important than the ECR in stabilizing high-index GaAs surfaces. Thus, our result is in accordance with the conclusions of this earlier study. Moreover, the low γ_f lends credibility for the (2×3) structural model proposed by Sauvage-Simkin et al. [33], Fig. 3b. The geometries obtained by optimizing our calculated structure are in good agreement with those determined by an analysis of the X-ray diffraction data (cf. Figs. 4 and 5; Table 3).

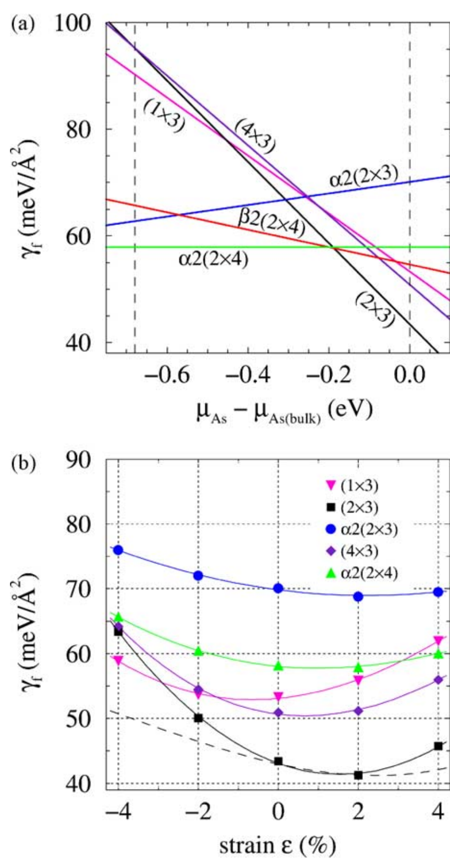

Fig. 4. Formation energy of $In_{2/3}Ga_{1/3}As(0\,0\,1)$ film with different reconstructions (a) as a function of μ_{As}; and (b) as a function of isotropic strain ε with respect to the GaAs substrate, and for $\mu_{As} = \mu_{As(bulk)}$. $\gamma_f(\mu_{As(bulk)})$ of the (2×4) reconstructions on panel (a) are obtained by interpolation to $\theta_{In} = 2/3$ ML. The effect of geometry relaxation for the (2×3) reconstruction is indicated by the dashed curve.

Another important feature of the pseudomorphic $In_{2/3}Ga_{1/3}As(0\,0\,1)$ film shows up upon considering γ_f as a function of the applied isotropic strain ε, here $\varepsilon = 0$ implies unstrained GaAs substrate. For small ε one can write γ_f in the form

$$\gamma_f(\varepsilon) = \gamma_f(0) + \mathrm{Tr}(\tau_{\alpha\beta})\varepsilon + \mathrm{O}(\varepsilon^2) \quad (2)$$

where $\tau_{\alpha\beta}$ is the intrinsic surface stress tensor [44].

The presence of the linear term $\tau_{\alpha\beta}$ is characteristic of a solid, and introduces the distinction between surface energy and surface stress, which is obsolete for liquid surfaces. The strain dependence of γ_f is calculated [45] in the range $\pm 4\%$, Fig. 4b. After the surface structures have been optimized once for the

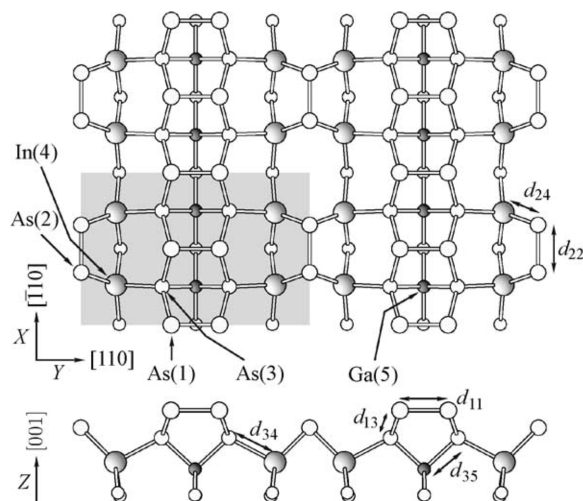

Fig. 5. Atomic structure and geometry parameters of the commensurate $In_{2/3}Ga_{1/3}As(0\,0\,1)$–$(2 \times 3)$ surface (see Table 3).

Table 3
Atomic coordinates and bond lengths as indicated in Fig. 5

Atom	LDA			GGA			XD				LDA [Å]	GGA [Å]	XD [Å]
	X	Y	Z	X	Y	Z	X	Y	Z				
As(1)	0.0	0.40	0.54	0.0	0.40	0.53	0.0	0.398	0.519	d_{11}	2.48	2.52	2.44
As(2)	0.34	0.0	0.39	0.35	0.0	0.38	0.343	0.0	0.384	d_{22}	2.45	2.50	2.51
As(3)	0.25	0.35	0.29	0.25	0.35	0.29	0.25	0.35	0.275	d_{13}	2.46	2.55	2.49
In(4)	0.26	0.15	0.07	0.26	0.15	0.06	0.267	0.151	0.063	d_{34}	2.68	2.82	2.69
Ga(5)	0.25	0.5	0.0	0.25	0.5	0.0	0.25	0.5	0.0	d_{35}	2.36	2.47	2.40
										d_{24}	2.59	2.71	2.63

X and Y are measured in units $2 \times a_0/\sqrt{2}$ and $3 \times a_0/\sqrt{2}$, respectively, while Z is given in units of the bulk lattice constant a_0 with respect to the Z coordinate of Ga(5). Experimental X-ray diffraction (XD) data are those reported by Garreau et al. [35] with an error bar of ± 0.004 for the in-plane coordinates, and ± 0.005 for the Z coordinate.

theoretical bulk lattice constant, further atomic relaxation of the strained slabs for small ε is expected to contribute to γ_f only to higher orders in ε. We confirm this behavior in our calculations for the (2×3) surface, which were performed both with and without strain relaxation (dashed and full line in Fig. 4). Because of the smallness of the effect on the slope at $\varepsilon = 0$, we have not considered it further for the other reconstructions. From the slopes at $\varepsilon = 0$ we infer that the dominant $\tau_{\alpha\beta}$ component for all reconstructions except (1×3) is *compressive*, $\mathrm{Tr}(\tau_{\alpha\beta}) < 0$; the As-rich reconstructions of GaAs(0 0 1) and InAs(0 0 1) are characterized [9] by $\mathrm{Tr}(\tau_{\alpha\beta}) > 0$. This is understood as to be due to the insertion of the indium atoms into the first cation layer, given that In–As bonds are obviously longer than Ga–As bonds. Clearly, the (2×3) reconstruction has the lowest formation energy over almost the entire range of strain. One can also note the apparent similarity in $\gamma_f(\varepsilon)$ for the α2-reconstructions; removal of the trench dimer from the $\alpha 2(2 \times 4)$ phase to form the cation-rich $\alpha 2(2 \times 3)$ does not lead to any significant change in the qualitative behavior. On the basis of the above results we single out the (2×3) reconstruction as the main subunit preferable of the $In_{2/3}Ga_{1/3}As$(0 0 1) film under As-rich conditions.

Interestingly, our calculations show that a perfectly ordered $In_{2/3}Ga_{1/3}As$(0 0 1) film is an excellent substrate for diffusion of In adatoms. The diffusion is strongly anisotropic, and the activation energies are substantially lower than their counterparts for Ga diffusion on the GaAs(0 0 1)–$\beta 2(2 \times 4)$ surface (see Table 1). Investigations about diffusion of In on disordered films are subject to ongoing work.

5. 2D–3D growth transition

For thicker films ($\theta_{In} > 1$ ML), the surface reconstructions displayed by the film become more similar to the known surface reconstructions of InAs. In particular, for most growth conditions, reconstructions with (2×4) symmetry reappear on the film. Only under very As-rich conditions (or, correspondingly, at low temperatures) the (2×3) reconstruction persists also for films thicker than 1 ML.

With increasing thickness, however, the heteroepitaxial strain built up in the film eventually drives it unstable. For InAs on GaAs(0 0 1), the leading instability is a growth mode transition from two-dimensional (2D) to three-dimensional (3D) growth which occurs spontaneously as soon as a critical thickness has been exceeded. Theoretically, we define the critical thickness by the requirement that the free energy of a homogeneous film becomes higher than the free energy of an ensemble of islands plus a correspondingly thinner film (overall conservation of the deposited material is implied) [39]. This definition is valid if local thermodynamic equilibrium between a 3D island and its surrounding wetting layer is established. Experimentally, different criteria have been used, e.g. the appearance of diffraction patterns characteristic of 3D structures in RHEED. The precise value of the critical thickness may depend an several factors, such as temperature, flux, and the number density of nucleated islands. Given the dependence on these factors, it is not surprising that a range of values, between 1.4 and 1.8 ML, is reported for the critical thickness of InAs films on GaAs [46].

An analysis of the thin film stability for larger θ_{In} on the basis of DFT calculations [9] has recently shown

that for most conditions, apart from very As-rich ones, the structural transition from (1 × 3) or (2 × 3) surface periodicity to (2 × 4) occurs prior to the 2D–3D growth mode transition. This finding is in accord with STM studies of MBE grown samples, where 3D islands on a (2 × 4) reconstructed wetting layer are observed [47,48].

6. Conclusion

In conclusion, we have discussed atomistic studies of island nucleation in MBE of GaAs. kMC simulations using rate constants derived from DFT calculations show that the β2-reconstruction of the GaAs(0 0 1) substrate acts as a template for the growth of a new layer of material. For ultra-thin films of InAs on GaAs, we have shown that surface alloying is a favorable process, and is associated with a triple-period reconstruction. In particular, a (2 × 3) reconstruction is identified as the most stable one for ideal perfectly ordered surfaces. The positions of the atoms in this structure are in excellent agreement with the analysis of experimental X-ray diffraction data. Upon further deposition, after the critical thickness is exceeded, the film will undergo a growth mode transition and spontaneously develop three-dimensional nanostructures. For a better understanding of this process, which is of considerable interest for the fabrication of self-assembled quantum dots, the effect of surface alloying must be taken into account. Our work shows a way how to analyze the kinetics and thermodynamics of the growth processes in InAs/GaAs(0 0 1) heteroepitaxy using results from first-principles DFT calculations.

Acknowledgements

We are thankful to Dr. T. Kita for communicating results prior to publication.

References

[1] G.R. Bell, M. Itoh, T.S. Jones, B.A. Joyce, Surf. Sci. 423 (1999) L280.
[2] C.T. Foxon, B.A. Joyce, Surf. Sci. 50 (1975) 434.
[3] B.A. Banse, J.R. Creighton, Appl. Phys. Lett. 60 (1992) 856.
[4] C. Sasaoka, Y. Kato, A. Usui, Appl. Phys. Lett. 62 (1993) 2338.
[5] N. Moll, A. Kley, E. Pehlke, M. Scheffler, Phys. Rev. B 54 (1996) 8844.
[6] W.G. Schmidt, S. Mirbt, F. Bechstedt, Phys. Rev. B 62 (2000) 8087.
[7] S.-H. Lee, W. Moritz, M. Scheffler, Phys. Rev. Lett. 85 (2000) 3890.
[8] W.G. Schmidt, Appl. Phys. A 75 (2002) 89.
[9] E.S. Penev, Ph.D. thesis, TU Berlin, 2002.
[10] C. Kumpf, D. Smilgies, E. Landemark, M. Nielsen, R. Feidenhans'l, O. Bunk, J.H. Zeysing, Y. Su, R.L. Johnson, L. Cao, J. Zegenhagen, B.O. Fimland, L.D. Marks, D. Ellis, Phys. Rev. B 64 (2001) 75307.
[11] M. Bockstedte, A. Kley, J. Neugebauer, M. Scheffler, Comput. Phys. Commun. 107 (1997) 187.
[12] J.P. Perdew, K. Burke, M. Ernzerhof, Phys. Rev. Lett. 77 (1996) 3865.
[13] C.T. Foxon, J. Vac. Sci. Technol. B 1 (1993) 292.
[14] Y. Garreau, M. Sauvage-Simkin, N. Jedrecy, R. Pinchaux, M.B. Veron, Phys. Rev. B 54 (1996) 17638.
[15] J.M. McCoy, U. Korte, P.A. Maksym, Surf. Sci. 418 (1998) 273.
[16] V.P. LaBella, H. Yang, D.W. Bullock, P.M. Thibado, P. Kratzer, M. Scheffler, Phys. Rev. Lett. 83 (1999) 2989.
[17] A. Ishii, T. Kawamura, Surf. Sci. 436 (1999) 38.
[18] C.T. Foxon, B.A. Joyce, Surf. Sci. 64 (1977) 293.
[19] C.G. Morgan, P. Kratzer, M. Scheffler, Phys. Rev. Lett. 82 (1999) 4886.
[20] P. Kratzer, M. Scheffler, Phys. Rev. Lett. 88 (2002) 36102.
[21] P. Kratzer, C.G. Morgan, M. Scheffler, Phys. Rev. B 59 (1999) 15246.
[22] M. Itoh, G.R. Bell, A.R. Avery, T.S. Jones, B.A. Joyce, D.D. Vvedensky, Phys. Rev. Lett. 81 (1998) 633.
[23] D.D. Vvedensky, M. Itoh, G.R. Bell, T.S. Jones, B.A. Joyce, J. Cryst. Growth 202 (1999) 56.
[24] M. Itoh, G.R. Bell, B.A. Joyce, D.D. Vvedensky, Surf. Sci. 464 (2000) 200.
[25] P. Kratzer, E. Penev, M. Scheffler, Appl. Phys. A 75 (2002) 79.
[26] G.R. Bell, T.J. Krzyzewski, P.B. Joyce, T.S. Jones, Phys. Rev. B 61 (2000) R10551.
[27] J. Krzyzewski, P.B. Joyce, G.R. Bell, T.S. Jones, Surf. Sci. 482–485 (2001) 891.
[28] J.G. Belk, C.F. McConville, J.L. Sudijono, T.S. Jones, B.A. Joyce, Surf. Sci. 387 (1997) 213.
[29] D.I. Westwood, Z. Sobiesierski, E. Steimetz, T. Zettler, W. Richter, Appl. Surf. Sci. 123–124 (1998) 347.
[30] T. Kita, K. Yamashita, H. Tango, T. Nishono, Physica E 7 (2000) 891.
[31] J.M. Moison, C. Guille, M. Bensoussan, Phys. Rev. Lett. 58 (1987) 2555.
[32] O. Brandt, K. Ploog, L. Tapfer, M. Hohenstein, R. Bierwolf, F. Philipp, Phys. Rev. B 45 (1992) 8443.
[33] M. Sauvage-Simkin, Y. Garreau, R. Pinchaux, M.B. Véron, J.P. Landesman, J. Nagle, Phys. Rev. Lett. 75 (1995) 3485.

[34] M. Sauvage-Simkin, Y. Garreau, R. Pinchaux, A. Cavanna, M.B. Véron, N. Jedrecy, J.P. Landesman, J. Nagle, Appl. Surf. Sci. 104–105 (1996) 646.
[35] Y. Garreau, K. Aïd, M. Sauvage-Simkin, R. Pinchaux, C.F. McConville, T.S. Jones, J.L. Sudijono, E.S. Tok, Phys. Rev. B 58 (1998) 16177.
[36] S. Ohkouchi, A. Gomyo, Appl. Surf. Sci. 130–132 (1998) 447.
[37] T. Nakayama, M. Murayama, in: Proceedings of the Fourth Symposium on Atomic-Scale Surface and Interface Dynamics, Tsukuba, 2000, p. 239.
[38] T. Kita, O. Wada, T. Nakayama, M. Murayama, Phys. Rev. B 66 (2002) 195312.
[39] L.G. Wang, P. Kratzer, M. Scheffler, N. Moll, Phys. Rev. Lett. 82 (1999) 4042.
[40] L.G. Wang, P. Kratzer, N. Moll, M. Scheffler, Phys. Rev. B 62 (2000) 1897.
[41] M.D. Pashley, Phys. Rev. B 40 (1989) 10481.
[42] L.G. Wang, P. Kratzer, M. Scheffler, Jpn. J. Appl. Phys. 39 (2000) 4298.
[43] L. Geelhaar, J. Marquez, P. Kratzer, K. Jacobi, Phys. Rev. Lett. 86 (2001) 3815.
[44] I.V. Marchenko, D.Y. Parshin, Sov. Phys. JETP 52 (1980) 129.
[45] G.-M. Rignanese, et al., Phys. Rev. B 52 (1995) 8160, Corrections to γ_f taking into account the change in the plane-wave basis set associated with the supercell volume change due to straining are introduced according to the scaling hypothesis.
[46] B.A. Joyce, D.D. Vvedensky, in: M. Kotrla, N.I. Papanicolaou, D.D. Vvendensky, L. Wille (Eds.), Atomistic Aspects of Epitaxial Growth, Kluwer Academic Publishers, Dordrecht, 2002, p. 301.
[47] N. Ikoma, S. Ohkouchi, Jpn. J. Appl. Phys. 34 (1995) L724.
[48] N. Grandjean, J. Massies, O. Tottereau, Phys. Rev. B 55 (1997) R10189.